LANDIS-II

Article

PnET-Succession v 5.1: Comprehensive description of an ecophysiological succession extension within the LANDIS-II forest landscape model

Eric J. Gustafson[1], Brian R. Miranda[1], Brian R. Sturtevant[1], Zaixing Zhou[2]

[1] Institute for Applied Ecosystem Studies, Northern Research Station, USDA Forest Service, Rhinelander WI, USA

[2] Earth Systems Research Center, University of New Hampshire, Durham NH, USA

Correspondence: Eric J. Gustafson, Eric.Gustafson@USDA.gov ORCID: 0000-0002-9506-3199

Abstract: The LANDIS-II forest landscape model simulates the successional response of forests to disturbances at landscape scale (10^4 – 10^8 ha). PnET-Succession is one of several succession extensions to LANDIS-II, and it is among the more mechanistic succession extensions. To increase its robustness for novel abiotic conditions and species assemblages, PnET-Succession includes many algorithms from the PnET-II forest ecophysiology model, which rely heavily on first principles of physiology, chemistry and physics. In the decade since PnET-Succession was originally coded, code revisions have accumulated to correct errors in logic, resolve discrepancies between PnET-II and PnET-Succession, and new code was added to enhance model capabilities. Consequently, current code is greatly altered compared to the original version, and the original description of the model in the literature no longer reflects the current model. In this paper, we describe in some detail the algorithms of PnET-Succession v5.1 to update the literature on PnET-Succession for greater transparency and as an easy-to-read companion to the open-source code. We conclude with ideas for future development of PnET-Succession and provide some examples of its use to explore likely forest landscape dynamics under novel (not yet empirically observed) conditions.

1. Introduction

Forest landscape models simulate forest dynamics at landscape scale (10^4 – 10^8 ha) as they respond successionally to disturbances. They have proved useful for generating insights into how disturbance regimes (including those directly and indirectly caused by human actions) interact with biotic and abiotic conditions to determine forest ecosystem change and resilience. Their strength is the ability to project the spatial pattern of forest state variables due to the successional response to spatially explicit simulation of disturbances coupled with spatial and temporal variation in the growing environment. Such models take a variety of modeling approaches, ranging from probabilistic state-and-transition models (e.g., VDDT-TELSA, RMLANDS) to process-based simulation models (e.g., LANDIS-II, Forest-BGCv2, iLAND) that use a mixture of phenomenological and mechanistic approaches to mimic the many processes that drive forest ecological dynamics (Gustafson 2013).

LANDIS-II (Scheller et al. 2007) is a forest landscape model simulating forest succession using the processes of forest development (seed dispersal, tree establishment, growth) and degeneration (disturbance, competition, senescence). LANDIS-II consists of a collection of extensions (modules) that can be individually activated to simulate the specific ecological processes that are important for the landscape being studied or the research (or management) question(s) being asked. Landscapes are represented as a grid of spatially interacting cells and vegetation is represented as species-age cohorts rather than individual stems to make the model tractable at landscape scale. On each cell,

species composition and vertical structure are assumed to be homogeneous and forest composition is represented as age cohorts of one or more tree species whose growth and competition are a function of their vital attributes (e.g., growth capacity, drought tolerance, shade tolerance, longevity, seed dispersal, ability to sprout vegetatively). The independent disturbance extensions (including silvicultural activity) simulate (usually spatial) processes that remove some or all of the tree species age cohorts as a function of disturbance type and severity and the susceptibility of the cohorts on each cell.

Each LANDIS-II simulation run requires a succession extension, and PnET-Succession (de Bruijn et al. 2014) is one of several available succession extensions, each having advantages (and various levels of complexity) for specific types of questions. Biomass Succession (Scheller and Mladenoff 2004) is a simple, yet powerful, succession extension that simulates growth and succession as a competition for "growing space" on each cell, with growth rate being a fixed species attribute (maximum Annual Net Primary Productivity (ANPP)). PnET-Succession is among the more mechanistic succession extensions. Many algorithms of the PnET-II forest ecophysiology model (Aber et al. 1992) were embedded in PnET-Succession to replace the more simplified and phenomenological functions of Biomass Succession. PnET-Succession simulates growth as a competition for light and water at a monthly time step with direct links to dynamic climate, including CO_2 concentration. As such, it is well-suited for questions involving novel abiotic and ecological conditions because it is based on physical and physiological first principles.

PnET-Succession was initially developed in 2012 by then post-doc Arjan de Bruijn, who developed the first draft of the extension as a proof of concept. In so doing, de Brujin showed that it was feasible to merge Biomass Succession and PnET-II. In essence, PnET-Succession simulates a single PnET-II "forest-type stand" for each cohort on each cell in each time step. However, unlike PnET-II, PnET-Succession needed to simulate multiple cohorts and species sharing light and water within a single cell. Since PnET-II simulates photosynthesis and water use on an entire grid cell, the PnET-Succession development team (de Bruijn, Gustafson, Miranda and Sturtevant) developed methods for multiple independent species-age cohorts to compete for light and soil water to simulate successional dynamics in LANDIS-II. The computing power available at the time required several simplifications and modifications of PnET algorithms to make the approach tractable for large landscapes with millions of cohorts. This approach replaced the loosely-coupled, metamodeling methodology of Biomass Succession (e.g., Xu et al. 2009) with directly-coupled relationships between abiotic drivers (climate, soil texture, CO_2) and growth and competition based on the logic of PnET-II, and this was expected to make it more robust to the novel environmental conditions (and species assemblages) expected in the future. PnET-Succession was developed for a study to project the likely outcome of attempts to reintroduce American chestnut to its former range in the central

Appalachian Mountains (USA) in the presence of novel insect pests and an altered future climate (Gustafson et al. 2018b)

One strength of this approach is that PnET-Succession models growth as a competition for light and water by simulating the physiology of photosynthesis rather than the more abstract competition for growing space that is used in Biomass Succession (Scheller and Mladenoff 2004). Furthermore, the links between abiotic drivers of growth, competition and stress are very direct, allowing a better signal between experimental treatments involving such drivers and forest landscape response. PnET-Succession also tracks many physiological state variables (e.g., foliage mass, multiple stress factors, carbon reserves, stomatal activity) that open possibilities for disturbance extensions to access or modify those variables directly (e.g., defoliating insects), with the landscape response being an emergent property of the mechanistic algorithms based on first principles.

In the decade since PnET-Succession was originally coded, computing power has increased and users and developers have uncovered various bugs, inefficiencies or undesirable simulated behavior, which in concert with the addition of code to add or improve model capabilities have resulted in a model whose code is greatly altered from the original version described in the literature (de Bruijn et al. 2014). In particular, the PnET-Succession development team worked with the PnET-II development team at the University of New Hampshire to make the extension more consistent with its parent ecophysiology model. In this paper, we describe in some detail the workings of the recently released version 5.1 (Gustafson and Miranda 2022a) to update the literature on PnET-Succession, to increase model transparency, and to provide a more direct companion to the open-source code (https://github.com/LANDIS-II-Foundation/Extension-PnET-Succession).

2. Conceptual design of PnET-Succession

The PnET-Succession Extension generally follows the methods of the LANDIS-II Biomass Succession Extension: species-age cohorts reproduce, grow (add biomass), age, and die. In PnET-Succession, elements of the PnET-II ecophysiology model of Aber et al. (1995) were embedded to simulate growth as a competition for available light and water, replacing the Biomass Succession algorithms that simulate a competition of cohorts for an abstract "growing space." PnET (Photosynthesis and EvapoTranspiration) is a simple, lumped parameter model of carbon and water balances of forest stands (Aber and Federer 1992), built on two principal relationships: 1) maximum photosynthetic rate is a function of foliar nitrogen concentration, and 2) stomatal conductance is a function of realized photosynthetic rate. PnET-Succession uses the photosynthesis and respiration equations from PnET-II to simulate photosynthesis in stacked canopy sublayers and allocation of photosynthates to specific cohort biomass components (root,

foliage, wood, non-structural carbon). Various stressors, respiration costs and biomass turnover (chronic loss from biomass pools) are simulated. The user-defined time step of PnET-Succession is used to control the frequency of outputs and the timing of its interaction with other extensions, but the internal time step of PnET-Succession is always monthly.

PnET-Succession simulates the competition of cohorts for water and light as a function of photosynthetic processes of each cohort (Figure 1). Competition for water is simulated on each site (grid cell) through a dynamic soil water balance that gains water through monthly precipitation (model input) and loses water each month (simulated) via runoff, interception, evaporation, percolation out of the rooting zone and consumption by cohorts through transpiration. Water balance is influenced by the specific soil and climate attributes associated with the biophysical unit (ecoregion) in which the cell is located. Competition for light is modeled by tracking (and attenuating) solar radiation through the canopy according to a standard Lambert-Beer formula.

For every month represented within a simulation year, PnET-Succession requires average daily maximum and minimum temperatures, total precipitation, average daily photosynthetically active radiation and atmospheric CO_2 concentration for each month as inputs; effects of ozone are optionally activated when monthly cumulative growing season ozone dose is also input.
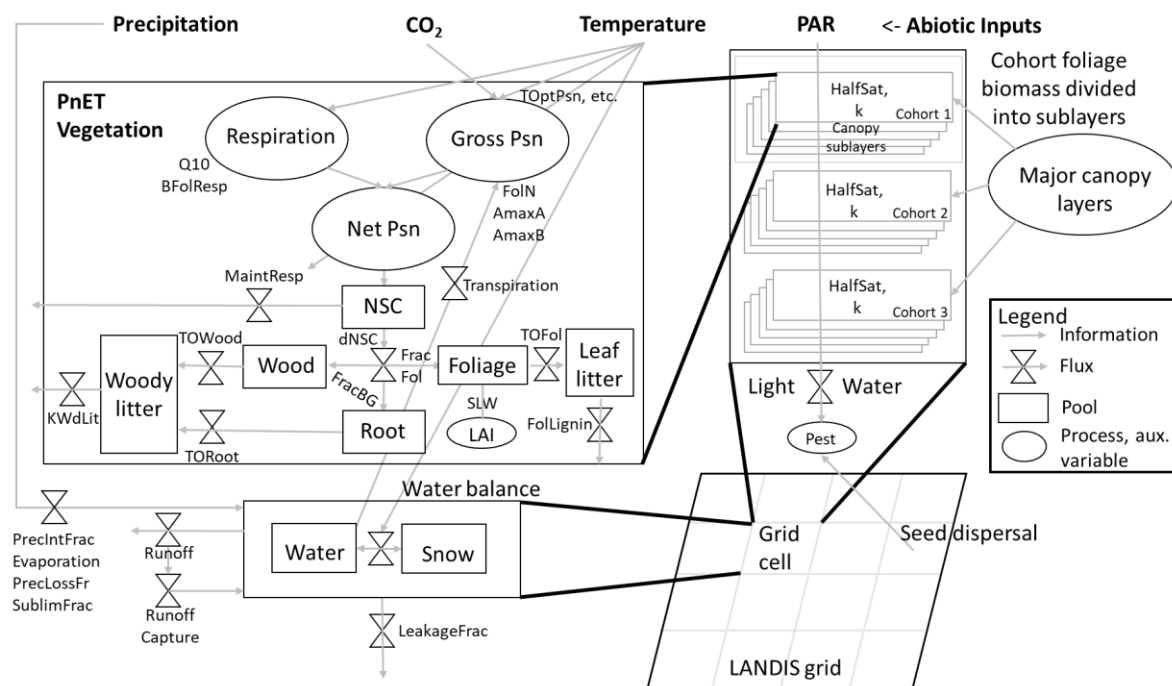

Figure 1. Conceptual design of PnET-Succession, which incorporates algorithms from the PnET-II model (Aber et al. 1995). Variables defined in Section 3. Adapted from de Bruijn et al. (2014).

3. Computational implementation of PnET-Succession

PnET-Succession modifies many algorithms and equations of PnET-II to make PnET-Succession tractable for landscape scales involving multiple cohorts on hundreds of thousands of landscape grid-cells over dozens to hundreds of years. The algorithms for each of the major cohort processes are described here in sufficient detail to provide a clear general picture of how the model works. A partial list of species life history and physiology parameters (and potential empirical sources for their values) is provided in the Appendix, and many parameters typically take standard defaults. Additional detail can be found in the open-source code (https://github.com/LANDIS-II-Foundation/Extension-PnET-Succession) and the User Guide (Gustafson and Miranda 2022a). There is also a spreadsheet available on the PnET-Succession page of the LANDIS-II website (https://github.com/LANDIS-II-Foundation/Extension-PnET-Succession/blob/master/deploy/docs/PnET-Succession%20function%20worksheet%20v5.0.xlsx) that graphs some of the functions that appear below, allowing users to experiment with various parameter settings to visualize their effect.

3.1 Photosynthesis

When multiple cohorts coexist on a single cell, they are organized into a hierarchical structure of canopy layers and sublayers. The entire cell canopy is represented by one or more major canopy layers, each shading the layers below. The method for allocating cohorts to canopy layers is described below (section 4.2), where each cohort is assigned to one of the major layers based on its size relative to other cohorts. Each individual cohort is subdivided into a user-specified number of sublayers (IMAX). Thus, PnET-Succession conceives of cohort canopies that are individually subdivided into sublayers and collectively aggregated into major canopy layers for the purpose of computing light attenuation as described in section 4.1.

Vegetation responses to environmental drivers are scaled from leaves to landscape grid cells using a "big-leaf" approach (Aber et al. 1992). The cohorts on each grid cell each have a dynamic biomass density of foliage, and each of the vertically stacked sublayers of foliage is conceptualized as a single "big leaf." Photosynthesis is explicitly simulated monthly for each sublayer (leaf), represented in the box labeled "PnET vegetation" in Figure 1. The photosynthetic outputs of each sublayer are summed to represent the productivity of the cohort, the attributes of the cohorts within a canopy layer are averaged (weighted) to represent the entire canopy layer (section 4.1), and all the canopy layers collectively represent the entire cell (section 4.3). The photosynthesis for each cohort canopy sublayer is simulated as described here.

NOTE. For the reader's convenience, input variables (parameters) are color-coded below. Species-specific input parameters appear in green, ecoregion parameters appear

in blue and global (or generic) parameters appear in purple. Variables appearing in black are typically dynamic state variables. Units are given in red.

The maximum net assimilation (i.e., conversion of carbon into photosynthates) rate of photosynthesis (Amax), as measured in laboratory experiments, is calculated as a function of foliar nitrogen (FolN) and modified by CO_2 concentration.

Amax = DelAmax * (AmaxA + AmaxB_CO2 * FolN))   [Units: nmole CO2/g Fol/s]

DelAmax is the CO_2 fertilization (enhancement) multiplier (defined below) and AmaxA and AmaxB (in the original PnET-II equation) are lifeform-specific intercept and slope coefficients relating FolN to Amax (Aber et al. 1996). Here AmaxB_CO2 is a modified form of input parameter AmaxB, optionally accounting for the level of CO_2.

AmaxB_slope = ((CO2AMaxBEff - 1.0) * AmaxB) / (550 – 350)

AmaxB_int = -1.0 * (((CO2AMaxBEff - 1.0) * 1.75) - 1.0) * AmaxB)

AmaxB_CO2 = AmaxB_slope *CO2 + AmaxB_int

CO2AmaxBEff is a user-defined (optional) parameter that determines the additional sensitivity of AmaxB to ambient CO_2 concentration (CO2) by defining the relative change in AmaxB at CO_2 concentration of 550 ppm, assuming AmaxB is defined for 350 ppm. The standard CO_2 fertilization effect (DelAmax) also includes an acclimation effect as described by Franks et al. (2013) and implemented here by Gustafson et al. (2018a):

DelAmax = $(C_i - \gamma) / (C_i + 2 * \gamma)*(C_{ref} + 2 * \gamma)/(C_{ref} - \gamma)$ [Units: proportional multiplier]

C_i is internal leaf CO_2 concentration, γ is the CO_2 compensation point, assumed to be 40 ppm based on an optimal temperature for photosynthesis of 25 °C, and C_{ref} is 350 ppm.

The instantaneous rate of foliar respiration (respiration cost of photosynthesis) is estimated as a user-defined proportion of Amax:

BaseFolResp = BaseFolRespFrac * Amax   [Units: nmole CO2/g Fol/s]

BaseFolResp is foliar respiration rate and the BaseFolRespFrac parameter is the proportion of photosynthates lost to respiration.

AmaxAdj = Amax * AmaxFrac   [Units: nmole CO2/g Fol/s]

GrossAmax = AmaxAdj + BaseFolResp   [Units: nmole CO2/g Fol/s]

AmaxFrac is the fraction of the early morning instantaneous photosynthetic rate (0.75) that represents mean daily photosynthetic rate and GrossAmax is maximum gross photosynthetic rate. This instantaneous rate is converted to a monthly gross photosynthetic production rate (RefGrossPsn) by:

RefGrossPsn = DaySpan * (GrossAmax * fDVPD * Daylength * MC) / 109
[Units: gC/g Fol/mo]

fDVPD = 1 – DVPD1 * VPD^DVPD2

DaySpan is number of days in the month, fDVPD is a vapor pressure deficit reduction (drought stress) factor (Aber and Federer 1992) calculated from species coefficients DVPD1, DVPD2 and the monthly vapor pressure deficit (VPD), Daylength is the length (hrs) of the middle day of the month (computed from latitude), and MC is the molecular weight of Carbon.

Potential gross monthly photosynthetic output (GrossPsnPotential) is computed by applying multiple reduction factors (Section 3.3) representing various stressors that reduce photosynthesis from its potential maximum (RefGrossPsn) using:

GrossPsnPotential = fRad * fTempPsn * fAge * RefGrossPsn * Fol   [Units: gC/m2 ground/mo]

fRad is the light stress reduction factor (see Section 3.3), fTempPsn is the temperature stress reduction factor, fAge is the age (senescence) reduction factor and Fol is foliar mass per unit of ground area.

Transpiration is computed by calculating the demand for water by GrossPsnPotential, the flux of CO_2 and H_2O influenced by vapor pressure deficit, accounting for stomatal sluggishness induced by elevated ozone concentrations (Gustafson et al. 2018a). Two fluxes (J) of molecules in and out of leaves (stomata) are used to compute transpiration in a more mechanistic (and dynamic) way than in PnET-II:

cicaRatio = (-0.075 * FolN) + 0.875   [Units: ratio (Ci/Ca)]

Ci = Ca * cicaRatio   [Units: ppm]

JCO2 = 0.139 * ((Ca - Ci) / V) * 0.000001   [Units: mol/cm²/s]

JCO2 is the flux of CO_2 into leaves, Ca is the ambient CO_2 concentration (CO_2 above), Ci is the CO_2 concentration inside the leaves, and V is the volume of air computed from monthly average minimum temperature using the ideal gas law. JH2O is the flux of water out of leaves, which is independent of the flux of CO_2, and given by:

JH2O = (0.239 * (VPD/V)) / ciModifier   [Units: mol/cm²/s]

VPD is vapor pressure deficit (calculated from temperature) and ciModifier is a modifier of gas conductance through stomata caused by stomatal sluggishness induced by ozone as determined by the species' tolerance to ozone. When ozone is not modeled (or 0 for any month), ciModifier is 1 and does not impact JH2O. Otherwise,

ciModifier = fWater + ((intercept + fWater * slope) * CumD40O3)

fWater is the water stress reduction factor (see section 3.3), CumD40O3 is the cumulative O_3 dose above a threshold concentration of 40 nmol/mol, and intercept and slope are coefficients that vary by ozone sensitivity classes (see Gustafson et al. 2018a).

The fluxes in and out of leaves are used to compute actual transpiration (loss of soil water through stomata) from GrossPsnPotential

PotentialTranspiration = 0.0015 * (GrossPsnPotential / (JCO2 / JH2O)) * CanopyLayerProp   [Units: mm water/mo] [//Constant is combined unit converter]

CanopyLayerProp is the proportion of the canopy layer that the cohort occupies (see section 4.1). PotentialTranspiration is compared to the quantity of water available in the soil, and if sufficient water is available, ActualTranspiration equals PotentialTranspiration.

AvailableWater = Water – SpeciesWiltingPoint   [Units: mm]

SpeciesWiltingPoint is the species-specific wilting point defined by the H4 parameter (see section 3.3). If AvailableWater is sufficient to meet the demand of PotentialTranspiration, then fWater is applied as the final reduction factor to calculate GrossPsn. Note that fWater can reflect stress from either too much water (waterlogging) or too little (drought) (see section 3.3).

GrossPsn = GrossPsnPotential * fWater [Units: gC/m2 ground/mo]

Actual Transpiration is calculated from PotentialTranspiration using the same reduction factor.

Transpiration = PotentialTranspiration * fWater   [Units: mm]

If PotentialTranspiration exceeds AvailableWater, then actual Transpiration equals AvailableWater, and GrossPsn is back-calculated to equal the photosynthesis that can be supported by the available water and fWater is then recalculated to be equal to Transpiration/PotentialTranspiration.

GrossPsn = (Transpiration / 0.0015) * (JCO2/JH2O) / CanopyLayerProp   [Units: gC/m2 ground/mo]

The instantaneous rate of foliar respiration (BaseFolResp) is converted to the monthly loss of carbon (RefFolResp) by:

RefFolResp = BaseFolResp * Q10Factor * DaySpan * (SecondsPerHour * 24) * MC /109   [Units: gC/g Fol/month]

Q10Factor is the Q-10 respiration factor (Mundim et al. 2020) and (SecondsPerHour * 24) is the number of seconds per day. Actual foliar respiration (FolResp) is based on the amount of foliage and determines net photosynthesis (NetPsn):

FolResp = RefFolResp * Fol   [Units: gC/m2 ground/mo]

NetPsn = GrossPsn – FolResp [Units: gC/m2 ground/mo]

The user can optionally invoke the acclimation of respiration rates (dynamic Q10-factor) to elevated temperatures as described by Wythers et al. (2013).

The PnET-II calculation of stomatal conductance to water vapor (gwv) was also modified for ozone impact (Gustafson et al. 2018a), after conversion of NetPsn units to µmolCO2/m2 fol/s as a function of leaf area (LAI):

netPsn_leaf_s = NetPsn * 1000000 * (1 / 12) * (1 / (Daylength * DaySpan)) * (1/LAI)
[Units: µmolCO2/m2 fol/s]

gwv=(netPsn_leaf_s*1.6*1000/(Ca−Ci))/(444.5−1.3667∗Tave)*10))   [Units: mm/s]

netPsn_leaf_s is the instantaneous rate of net photosynthesis and Tave (°C) is average monthly temperature (Tmax+Tmin)/2. See Gustafson et al. (2018a) for the calculation of O3Effect using gwv, which then modifies NetPsn:

NetPsn = NetPsn * O3Effect   [Units: gC/m2 ground/mo]

GrossPsn = (ActualTranspiration / 0.0015) * (JCO2/JH2O) / CanopyLayerProp
[Units: gC/m2 ground/mo]

3.2 Foliage

In PnET-Succession, leaf area index (LAI) is estimated for each cohort in each major canopy layer, and available light is computed for each major layer and each sub-layer within each canopy layer, and for the sub-canopy (i.e., ground). LAI is calculated from the cohort foliage mass using the specific leaf weight (SLW$_{max}$) of the species. Within a cohort canopy, the effective SLW$_i$ of a sublayer changes from the top sublayer to the bottom if SLW$_{Del}$ >0:

$$SLW_i = SLW_{max} - SLW_{Del} \times \frac{i}{IMAX} \times Fol$$

SLW$_{max}$ and SLW$_{Del}$ are leaf weight (thickness) parameters, i is the sublayer index (top sublayer i =0), IMAX is the number of sublayers per cohort, and Fol is the cohort foliage mass (g/m^2).

$$LAI_i = \frac{Fol}{IMAX} \div SLW_i$$

Cohort LAI is the sum of these sublayer LAI$_i$ values.

Several modifications were made to PnET algorithms regarding foliage and canopy layering to make them tractable at landscape scales, primarily by broadening the scale of integration operations (de Brujin et al. 2014). (1) The timestep was broadened from the daily PnET timestep to monthly. (2) The number of sub-layers within a cohort canopy (IMAX) was 50 in PnET (which has been acknowledged as excessive, S. Ollinger pers. comm.), but in PnET-Succession is set by the user (typically=5) to increase computational efficiency, where each sub-layer represents an equal proportion of the total foliage mass within the cohort's canopy. (3) The original PnET adds foliage to successively lower canopy sublayers until there is insufficient light to produce a positive carbon balance. This is computationally time-consuming and difficult with multiple canopy layers. Therefore, PnET-Succession allocates cohort foliage in proportion to the active wood (xylem) that supports that foliage, and the amount of light (and water) available to each sublayer determines the relative productivity of that foliage. Cohort carbon reserves become depleted if there is insufficient light to cover respiration costs. (4) Cohort biomass in PnET-Succession is used as a surrogate for tree height to determine the major canopy layer of each cohort, and major canopy layers are added when the variation in biomass among cohorts exceeds a user-defined threshold (LayerThreshRatio). (5) Cohort photosynthates in PnET-Succession are allocated to four pools (foliage, root, wood and non-structural carbon (reserves, NSC)). Net photosynthesis is initially allocated to the NSC pool, and allocations to the other pools occur annually or seasonally. Maintenance respiration costs are covered monthly, wood and root biomass are allocated at the end of the year such that the above- and below-ground biomass ratio is preserved, and foliage is allocated at the start of the growing season and following foliage loss to disturbance. (6) Cohorts die if the NSC pool is depleted (ratio of NSC to active wood <0.01) at the end of a year.

Light (photosynthetically active radiation or PAR) is consumed as it travels through each canopy sublayer of a cohort as a function of the sublayer's proportion of cohort LAI and the species' foliage extinction coefficient (k).

For each canopy sublayer,

LightBelow = LightAbove * $e^{(-k*sublayerLAI)}$ [Units: radiation units are input as either Watts/m2 or µmol/m2/sec]

LightAbove is the radiation entering the canopy sublayer from above and LightBelow is the radiation exiting from the bottom of the canopy sublayer.

3.3 Reduction (stress) factors

PnET-Succession computes a monthly maximum theoretical photosynthesis rate (GrossAmax) for a cohort based on the foliar nitrogen content of leaves as described above. GrossAmax is reduced in each month by the state of each stress factor (water,

light, temperature, ozone and age (senescence)). This is done by computing a reduction factor (multiplier that ranges from 0 to 1) for each stressor based on the level of that stressor as experienced by the cohort in the current month. GrossAmax is multiplied by all the reduction factors to compute actual gross photosynthetic rate (GrossPsn). There is also an enhancement multiplier for elevated CO_2 (DelAmax, see above), which is greater than 1 when CO_2 concentration exceeds the reference concentration (350 ppm) and can serve to increase Amax in response to "CO_2 fertilization" (Section 3.1).

Soil water potential is simulated independently on each cell using a "leaky bucket" model that depends on the holding capacity of the bucket (soil texture and soil depth) and the relative saturation of the soil caused by the dynamic monthly gains and losses of water. Inputs include precipitation and snowmelt, and losses come from interception, runoff, leakage, evaporation, and transpiration (in that order). Horizontal flow of water above- or below-ground is not modeled.

The proportion of precipitation that is attributed to snow is calculated from average monthly air temperature (Tave=(TMin+TMax)/2), and immediately reduced by sublimation as a function of SnowSublimFrac:

NewSnow = Precip * Max(0,Min(0,(Tave – 2)/-7)) * (1-SnowSublimFrac) [Units: mm water equivalent]

Snowmelt is constrained to a rate of 2.74 mm per degree day (USDA NRCS 2004):

SnowMelt = SnowPack * 2.74 * Max(0, Tave) * DaySpan

Interception is calculated as a function of LAI and the ecoregion parameter PrecIntConst:

Interception = Precip * (1 – e^(-1 * PrecIntConst * LAI) Units: mm/mo

Runoff is incoming water to the soil that exceeds the saturation capacity of the soil (and RunoffCapture if used). Leakage is a proportional amount of the water in excess of field capacity (water content when pressure head = -33 kPa).

Leakage = LeakageFrac * (Water – FieldCap) Units: mm/mo

The evaporation term is used to represent both direct soil water loss to the atmosphere and the use of water by plants that are not modeled as tree cohorts (shrub/herbaceous transpiration). Both processes are considered to have access to soil water to a depth that may be less than the full soil depth, so evaporation is constrained by EvapDepth. Potential evaporation is calculated from Hamon (1961) based on temperature and day length:

es = 6.108 * e^((17.27 * Tave) / (Tave + 237.3))

RET= 1.2 * 0.165 * 216.7 * daylength/12hr * (es/(Tave + 273.3)) Units: mm/day

The reference evaporation (RET) is diminished by shading as determined by canopy LAI.

PotentialEvap = RET * e^(-ETExtCoeff * LAI) * DaySpan Units: mm/mo

ActualEvap = Min(PotentialEvap, Water * EvapDepth) Units mm/mo

ETExtCoeff is a canopy extinction coefficient used to reduce soil water evaporation as LAI increases.

Water stress – either from too little (drought) or too much (waterlogging) water – occurs through a variety of mechanisms that ultimately limit photosynthesis, transpiration, or both (Menezes-Silva et al. 2019). Drought and waterlogging tolerant species each have traits that allow the species access to resources, or minimize/repair damage, generally via carbohydrate investments (Kreuzwieser and Rennenberg 2014, Brodribb et al. 2020). Rather than model such a diversity of processes explicitly, PnET-Succession applies a phenomenological approach to water stress according to basic theory on trade-offs between growth rate and stress tolerance (Huston and Smith 1987). A water reduction factor (fWater) is determined for each species found on the cell by comparing the current soil water potential of the cell to the parameters defining the tolerance of the species to waterlogging (H1, H2) and drought (H3, H4) (H1-H4; Figure 2). H2 is the water potential above which photosynthesis begins to slow due to waterlogging and H1 is the water potential above which photosynthesis ceases because of waterlogging. H3 is the water potential below which photosynthesis begins to slow due to drought stress and H4 is the water potential below which photosynthesis ceases because of drought. Soil water potential in PnET-Succession is computed as absolute value of pressure head (m) and thus, H1-H4 are positive numbers. The code reads:

if (pressurehead <= H1) fWater = 0 [//extreme waterlogging]

else if (pressurehead >= H4) fWater = 0 [// extreme drought]

else if (pressurehead > H3) fWater = 1 - ((pressurehead - H3) / (H4 - H3)) [//some drought]

else if (pressurehead < H2) fWater = (1.0/(H2-H1))*pressurehead - (H1/(H2-H1)) [//some waterlogging]

else fWater = 1 [//no water stress]

When fWater=1.0, there is no water stress, and the multiplier causes no reduction in photosynthesis (as is true for all reduction factor multipliers).
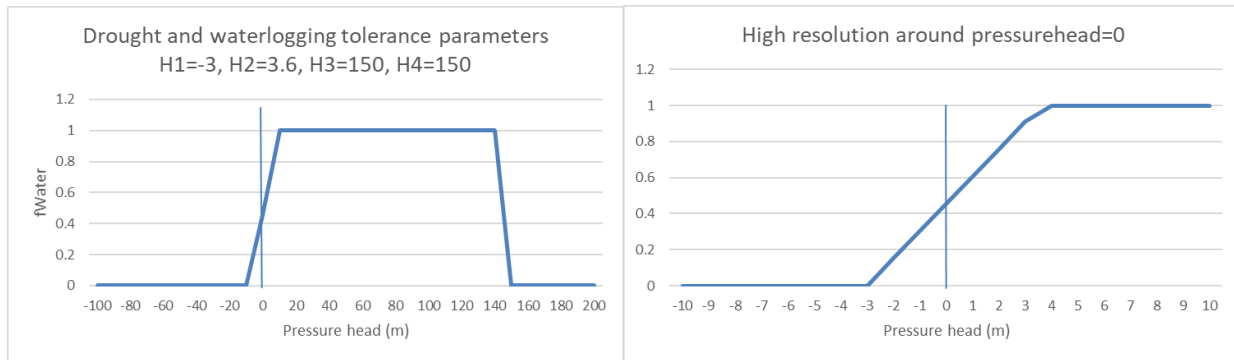
Figure 2. Illustration of the relationship of waterlogging and drought tolerance parameters (H1-H4) to water stress (fWater) across a spectrum of soil water potential. Panels show water stress from waterlogging when pressure head <3.6 m and from drought when pressure head >150 m, and no water stress reduction when pressure head is between 3.6 and 150 m. This example reflects the physiological reality that trees are not water stressed until water potential drops below their threshold for water absorption (H4). This hypothetical species has moderate waterlogging tolerance because H1 is negative (-3), allowing fWater to be non-zero even when soils are supersaturated (pressure head=0).

Incoming precipitation is divided into equal discrete precipitation events within a month, with the number of monthly events set as an ecoregion parameter. Precipitation from individual events is stochastically assigned to individual canopy sublayers among all cohorts on the cell, with some sublayers potentially receiving multiple events and others receiving none (in a given month). This random assignment ensures that all sublayers (and cohorts) have equal priority (over time) to incoming water. However, cohort processing begins with the top main canopy layer, so the largest cohorts will have first priority access to water already in the soil. Because water stress experienced by each species is dynamic (monthly) and dependent on its water tolerance parameters (H1-H4), some species will become water-stressed before others as water potential drops. Eventually, some may be unable to access any water if the cell water potential drops below their H4 value. Any water remaining in the soil after a sublayer is processed is available to subsequent sublayers.

Light stress (fRad) is modeled based on the amount of photosynthetically active radiation (PAR) reaching canopy sublayer (*i*) and the shade tolerance (HalfSat) of the species:

$$\text{fRad} = 1 - e^{-PAR_i \frac{\log(2)}{HalfSat}}$$

PAR_i is determined by the amount of light impinging on the top of the canopy and its extinction as it travels down through the canopy (Lambert-Beers law), and HalfSat (half-

saturation point) is the radiation at which photosynthetic rate is half of its maximum value, i.e., fRad = 1/2 (Jassby and Platt 1976).

The temperature reduction factor (fTemp_Psn) controls the photosynthesis rate reduction caused by suboptimal temperature, and is computed by the parabolic curve:

$$\text{fTempPsn} = \frac{(PsnT_{max} - T_{day}) \times (T_{day} - PsnT_{min})}{((PsnT_{max} - PsnT_{min})/2)^2}$$

Tday is the mean daytime temperature for the current month and PsnTmin and PsnTmax are the species-specific minimum and maximum (respectively) temperatures where photosynthesis stops. Note that the units of these temperature values (Tday) are the mean daytime (sunlit hours) temperatures and not the temperature related to instantaneous photosynthetic rate. Tday = ((Tmin+Tmax)/2). When the DTEMP option is not used (false), fTempPsn equals 1.0 when Tday is at or above the species parameter PsnTOpt (optimal temperature for photosynthesis), and the equation above applies only for temperatures below PsnTOpt. Using the DTEMP option (default), fTempPsn declines parabolically towards zero as temperatures deviate in either direction from PsnTOpt, as it does in PnET-II. If PsnTMin and PsnTMax are not equidistant (in degrees C) from PsnTOpt, the parabolic curve is asymmetrical. If PsnTMax is not supplied by the user, it is estimated using PsnTmax = PsnTOpt + (PsnTOpt − PsnTmin).

Unlike in Biomass Succession, cohorts do not deterministically die at longevity age. The age reduction factor adds an extra stressor to ensure that cohorts cannot exceed their longevity age:

$$fAge = 1 - (Age/longevity)^{PsnAgeRed}$$

fAge is the senescence reduction factor, Age is cohort age, longevity is the species longevity parameter and PsnAgeRed is a shape parameter that controls the shape of the curve relating age to fAge. fAge becomes zero when the cohort reaches longevity age, but cohorts that are stressed by other factors will die before reaching longevity age, with PsnAgeRed helping to determine how soon before longevity age they die. Note that photosynthetic capacity does not empirically decline as trees age – this reduction factor's sole purpose is to ensure that cohorts senesce and die no later than their longevity age.

3.4 Allocation

The monthly photosynthetic carbon output of a cohort is temporarily stored in the non-structural carbon (NSC) pool. A species-specific fraction of NSC (relative to active biomass) is held in reserve to cover monthly maintenance respiration costs and to build future foliage. Allocation from the NSC pool to foliage occurs at the start of the growing season and allocation to the wood and root pools occurs at the end of the year, each involving a conversion from carbon to dry-weight biomass. A target foliage biomass allocation is computed based on the estimated amount of active wood (xylem tissue) and

the species-specific fraction of active wood that determines the size of the foliage pool (FracFol). The actual foliage allocation equals the target foliage mass unless the cohort is stressed such that insufficient NSC reserves are available. Available NSC at the end of the year is allocated to wood and root biomass to maintain the target wood:root ratio (FracBelowG). A cohort dies if it is unable to maintain sufficient NSC reserves (i.e., the ratio of NSC to active biomass ≤0.01 because of inadequate productivity due to stress) at the end of a year (prior to allocation to wood and roots).

3.5 Seasonality

Growing season length is dynamic and is controlled in PnET-Succession by a species-specific temperature threshold. Growing season for a species starts (foliage is added and photosynthesis is simulated) in the month when Tmin first exceeds the species threshold (LeafOnMinT) and ends (foliage is shed and photosynthesis is halted) in the month when Tmin drops below that threshold. If the surface of the soil profile is frozen (can only happen if SoilIce=true) in any month of the growing season (possible in high latitudes), fWater will equal 0 (i.e., no photosynthesis), no foliage will be added in that month, but any existing foliage will be retained until the month when Tmin drops below LeafOnMinT.

3.6 Establishment

Establishment of new cohorts is modeled as a two-step process: 1) seed dispersal and 2) establishment (recruitment) of a viable cohort. Seed dispersal determines which species have propagules arriving at each cell and this is handled by the LANDIS-II Succession Library (common to all succession extensions) as a function of two seed dispersal distance parameters (see LANDIS-II Model v7.0 Conceptual Description). Establishment itself is regulated in part by two user-defined species-specific scaling parameters (EstRad and EstMoist; range=0.0-1.0) that can be used to simulate the sensitivity of establishment to water and light. Light and water can have a user-defined weight when computing the probability of establishment (Pest) for a species. MaxPest is a universal scaling parameter that can be used to tune establishment rates of all species together (see PnET-Succession User Guide (Gustafson and Miranda 2022a) for specifics). A new cohort is established if propagules are present on the cell and a uniform random deviate ≤Pest is generated. Initial biomass for a successfully established cohort is computed for a 1-year-old cohort of the species based on InitialNSC and cohort carbon allocation rules. This initial cohort is grouped ('binned') appropriately into a broader cohort (e.g., age 1 – 10) at the next succession time step.

4. New features in PnET-Succession v.4 and v.5

4.1 Accounting for canopy gaps

Revisions were made in v.5 to better estimate the total biomass on cells with multiple cohorts. In light of the empirical evidence that tree crowns typically exhibit almost no spatial overlap (canopy shyness, Hajek et al. 2015), a useful conceptual model of a PnET-Succession canopy (potentially including multiple cohorts) (Gustafson et al. inreview) is to imagine that the canopy portion of each cohort on a cell can be represented as a cube (i.e., all the individual crowns of a cohort are collected into a single conceptual cube). Thus, a major canopy layer is made up of all the side-by-side cubes of similar-sized cohorts (because biomass is a surrogate for height) and suspended above the cell, with the relative horizontal dimension of each cube being proportional to cohort occupancy within the cell (Figure 3). Multiple major canopy layers (each composed of similar-sized cohorts) are stacked, with each cohort within a layer receiving the same intensity of incoming light from above. This simplification of canopy structure is similar in kind to the "perfect plasticity approximation" applied to the canopy structure within certain cohort-based dynamic global vegetation models (e.g., Weng et al. 2015, Fisher et al. 2018). If a cohort dies or is disturbed, the horizontal dimensions of its "cube" are reduced, creating "open space" that could be filled by other cohorts (see below). The proportional size (PCanArea) of cohort i's cube is computed as current leaf area index (LAI) of the cohort relative to its maximum LAI (MaxLAI), which is provided either as a specific species parameter or estimated from other species parameters. When MaxLAI is calculated from parameters, it uses the LAI equations in section 3.2, but instead of uses the Fol variable, it uses estimated maximum foliage mass (PeakFoliage), which is derived from species parameters FrActWd and FracFol:

$$PeakFoliage = \left(\frac{1}{FrActWd}\right) \times FracFol \times e^{(-1)}$$

The calculation of PCanArea assumes that a canopy cube could completely fill a cell (proportion = 1) when its cohort reaches its maximum LAI.

$$PCanArea_i = \frac{LAI_i}{MaxLAI_i}$$

The proportion of a major canopy layer on a cell that is occupied by cohort canopy cubes (PCanAreaLayer) is the sum of the proportion of the cohort canopy cubes in the layer.

$$PCanArea_{Layer} = \sum_{n}^{i} PCanArea_i$$

A major canopy layer is considered filled (all cubes have expanded horizontally to eliminate all gaps) when the sum of cohort proportions ≥ 1. Because of the assumption of non-overlapping cohort canopies within a layer (Hajek et al. 2015), the sum of the proportional canopy areas is further constrained not to exceed 1. If PCanArea$_{Layer}$ is greater than 1, then PCanArea(i) for each cohort is proportionally rescaled to make PCanArea$_{Layer}$ equal 1.

$$PCanArea_i = PCanArea_i / PCanArea_{Layer}$$

However, this limitation that constrains a cohort's horizontal spread may be unrealistic when the constraint is applied abruptly as if stem exclusion mortality is instantaneous when cohorts experience altered competition when a new cohort enters or leaves a canopy layer. An optional generic parameter (CanopySumScale) can be used to scale the rate at which the constraint that cumulative canopy proportions cannot exceed 1 is applied (i.e., the rate of stem exclusion mortality). When CanopySumScale = 1, the constraint is abruptly applied (i.e., PCanAreaLayer is never allowed to exceed 1), and behaves as described above. When CanopySumScale <1, the constraint is gradually applied at a rate proportional to CanopySumScale, and when CanopySumScale =0, there is no constraint. Thus, CanopySumScale indicates the relative rate at which excess canopy proportion is removed. The canopy proportion for each cohort is calculated once each simulation year, so CanopySumScale represents the annual rate of stem exclusion mortality.

$$PCanArea_i = \left(\frac{PCanArea_i}{PCanArea_{Layer}} - PCanArea_i \right) * CanopySumScale + PCanArea_i$$

Once a cohort's canopy proportion has been rescaled in this way, the proportion becomes capped at that level for the remainder of that cohort's existence. This limitation reflects the assumption that once canopy closure has been reached, a cohort cannot expand its canopy horizontally by new stem or branch growth. Therefore, if a cohort dies or loses part of its biomass prior to canopy closure, any 'space' that was occupied by its lost canopy becomes 'open' and the 'open' space can only be gradually refilled by the impacted cohort (for example, as in a thinning treatment), or if "released" cohorts in lower canopy layers increase enough biomass to join the higher canopy layer, leaving a gap in their former canopy layer (see section 4.2 below). Similarly, if a cohort dies after canopy closure (PCanArea_Layer = 1), the 'open' space in that layer can only be filled by cohorts growing up into that layer, as the other cohorts in that layer are limited in their ability to expand into that canopy space.

Light travels downward through the sub-layers of each cube independently and each sub-layer consumes light according to the LAI and extinction coefficient (k) of the cohort's foliage.

$$Transmissivity_i = e^{-k*LAI_i}$$

The "open" space experiences no light attenuation because its LAI is zero. Light exiting the bottom of each canopy layer is the proportionally weighted average of the light exiting from all the side-by-side cubes, taking into account the 'open' proportion.
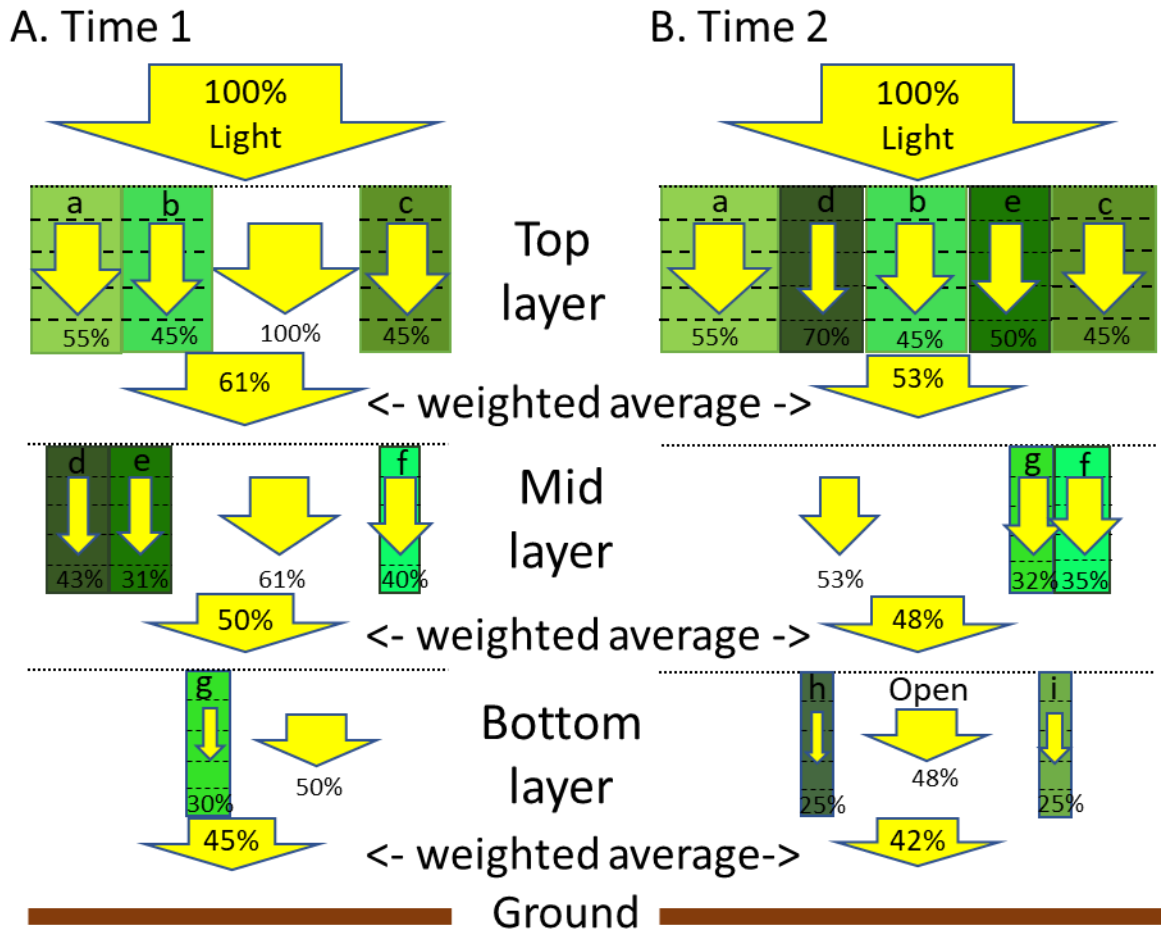
Figure 3. Diagram of the conceptual logic of algorithms for processing light dynamics in cohort canopies. Panel A illustrates canopy layering of cohorts on a hypothetical grid cell, and Panel B shows the altered canopy configuration after many years of growth and establishment. The crowns of all the trees in a cohort are represented as a single rectangle (cube) whose width is proportional to cohort size (biomass). Canopy cube sublayers are delineated by dotted lines. The percentage of sunlight transitioning through major canopy layers is given and represented by the width of the yellow arrows, determined by the LAI and extinction coefficient of the species' foliage in each cube. "Open" space represents all unoccupied "gaps" in the major canopy layer (no foliage). Light exiting all cohort cubes in a major canopy layer is averaged, weighted by canopy proportion, to determine the light available to all cohorts in the next lower major canopy layer. Note that if the gap in the top major canopy layer at Time 1 was caused by disturbance after crown closure had been achieved, then cohorts a-c would be constrained to the same growing space (no increase in "cube" width) in subsequent time steps.

When CanopySumScale < 1, a canopy layer with multiple cohorts can temporarily exceed a total canopy proportion of 1. When this happens, the simple proportionally weighted average of light attenuation is not a good representation of the light reaching

the layer below. When the sum of PCanArea$_i$ > 0, the total light attenuation through the layer is calculated as:

$$Transmissivity_{Layer} = \prod_i Transmissivity_i^{PCanArea_i}$$

PAR reaching the layer below is then PAR * Transmissivity$_{Layer}$.

4.2 Canopy layering

As described above, a major canopy layer is conceptualized as a collection of side-by-side cohort "cubes," in which the cohorts occupy canopy area (i.e., PCanArea$_i$) proportional to their respective biomass and maximum LAI. The simplifying assumption is that all cohorts within a layer receive the same intensity of incoming light (i.e., all light is received from above). But when there are cohorts of markedly different sizes on a cell, they are assigned to different major canopy layers and such layers (made up of collections of side-by-side cubes) are stacked (Figure 3). The algorithm that assigns cohorts to major canopy layers was simplified in v.5.1 (Gustafson et al. in review). The user specifies the maximum number of allowable major canopy layers (MaxCanopyLayers) as a generic parameter and cohorts are assigned to different canopy layers if their maximum lifetime woody biomass differs by more than the proportion set in the generic parameter LayerThreshRatio. For example, if LayerThreshRatio is 0.667, then a cohort's biomass must be less than two-thirds of the biomass of a larger cohort to be placed in a lower layer than the larger cohort. Cohorts are processed from biggest to smallest so that when MaxCanopyLayers limits the number of canopy layers, the smallest cohorts are lumped together rather than the largest. If there is insufficient variation in biomass among cohorts, the number of assigned layers may be less than MaxCanopyLayers. The layering algorithm uses the cohort maximum lifetime biomass (see end of next section) to account for cases where a large cohort (assumed to have a tall height) is partially disturbed or begins to senesce, causing a reduction in its biomass. This rule reflects the reality that senescence or partial damage to cohorts generally results from loss of individuals (density) rather than decrease in height. For canopy layering, using the maximum lifetime biomass allows the algorithm to treat those cohorts as maintaining their canopy position (i.e., height).

Cohorts within a canopy layer compete for canopy space (2-dimensional horizontal) but their vertical volume (LAI) increases proportionally with their canopy area to a maximum defined by their species' MaxLAI (see Section 4.1). Total LAI for the cell is calculated as the sum of the layer LAIs, with each layer LAI being the proportional sum of the LAI of the cohorts within the layer.

$$LAI_{Layer} = \sum_n^i PCanArea_i \times LAI_i$$

$$LAI_{Cell} = \sum LAI_{Layer}$$

Light that exits the bottom-most major canopy layer is assumed to reach the ground and be available to establishing cohorts.

4.3 Scaling biomass estimates

The conceptualization of tree species cohort canopies acting as non-overlapping cubes within a layer means that the woody biomass supporting those cubes is also restricted to a subset of the area within the cell (Gustafson et al. in review). PnET-Succession therefore computes biomass in units that represent a biomass density (gDW/m²) within their cohort space (cube). Prior versions of PnET Succession assumed that all cohorts equally (and simultaneously) occupy the entire space of the cell, so this new assumption of non-overlapping canopies within a layer is a significant change that requires a shift in the underlying logic governing biomass-size assumptions. In general terms, cell-level estimates of all cohort attributes are computed according to the proportion of the cell area that the cohort occupies, with that proportion estimated by PCanArea. Thus, a cohort biomass density estimate represents the cohort's density wherever it (i.e., individual trees) is found on the cell and the cell-level biomass density estimate represents the cohort's average density across all of the cell's area (i.e., including both where its individuals ARE found and where they are NOT found).

Some examples will help illustrate the logic and consequence of this new approach. Consider a cell that carries 10,000 g/m² of cohort biomass density in one cohort, and 3,000 g/m² of cohort biomass density in another cohort (see example A in Table 1). Applying a LayerThreshRatio of 0.5 would separate the two cohorts into separate canopy layers, a top layer with 10,000 g/m² cohort biomass density and a lower layer with 3,000 g/m² cohort biomass density. In this example, the top layer is fully occupied, but the lower layer is only 57% occupied because its LAI is less than its maximum LAI, meaning that 43% of the cell area is 'open' in this lower layer. The cell-level biomass density is the sum of the cohort biomass density of the two layers: 11,714.3 g/m² biomass (i.e., 10,000 + (3,000 * 0.57)). Compare that situation with one having two cohorts with 10,000 g/m² cohort biomass density, and a third with 3,000 g/m² cohort biomass density (Example B in Table 1). The layering algorithm will place the two cohorts with 10,000 g/m² cohort biomass density into the top canopy layer, and the cohort with 3,000 g/m² cohort biomass density into a lower layer. In this example, the two larger cohorts each have a canopy cube width equal to half the width of the cell. Their cohort biomass density of 10,000 g/m² exists on the portion of the cell occupied by their foliage, but since their canopies each occupy only half of the cell, the biomass density of each individual cohort when scaled to the entire cell area is 10,000*0.5=5,000 g/m². But the weighted average for the entire layer (i.e., over the entire area of the cell) is the sum of their cell-level biomass density, or 10,000 g/m². In the lower layer there is just one cohort with a cohort biomass

density (3,000 g/m²), but because it occupies just 57% of the cell, its cell-level biomass density is 1,714.3 g/ m², and because it is the only cohort in the layer, the cell-level layer biomass density is also 1,714.3 g/ m².

The total cell-level biomass density is equal to the sum of the biomass densities of both major canopy layers (i.e., 11,714 g/ m²).

In these examples, at least one canopy layer is fully occupied (i.e., canopy closure has been reached and there is no open space within that layer). Examples C and D (Table 1) show the computations when there is open space (PCanArea(i) <1.0) in all layers due to mortality (Example C) or partial disturbance (Example D) affecting Cohort 2 from the condition that was represented in Example B. Note that canopy layer biomass density is always computed as a weighted average of each cohort in the layer (weighted by PCanArea) and total cell biomass density is the sum of the layer densities.

Table 1. Illustrative examples of how cell-level biomass scaling and canopy layering are computed.

Example A	Cohort Biomass Density (g/m2)	Layer	LAI	MaxLAI	Adjusted PCanArea	Cell Biomass Density (g/m2)	Layer Biomass Density (g/m2)
Cohort 1	10000.00	Top	3.50	3.50	1.00	10,000.00	10,000.00
Cohort 2	3000.00	Bottom	2.00	3.50	0.57	1,714.29	1,714.29
					Cell Total Biomass Density (g/m2):	11,714.29	11,714.29

Example B	Cohort Biomass Density (g/m2)	Layer	LAI	MaxLAI	Adjusted PCanArea	Cell Biomass Density (g/m2)	Layer Biomass Density (g/m2)
Cohort 1	10000.00	Top	3.50	3.50	0.50	5,000.00	-
Cohort 2	10000.00	Top	3.50	3.50	0.50	5,000.00	10,000.00
Cohort 3	3000.00	Bottom	2.00	3.50	0.57	1,714.29	1,714.29
					Cell Total Biomass Density (g/m2):	11,714.29	11,714.29

Removal Cohort 2

Example C	Cohort Biomass Density (g/m2)	Layer	LAI	MaxLAI	Adjusted PCanArea	Cell Biomass Density (g/m2)	Layer Biomass Density (g/m2)
Cohort 1	10000.00	Top	3.50	3.50	0.50	5,000.00	-
Cohort 2	0.00	Top	0.00	3.50	0.00	0.00	5,000.00
Cohort 3	3000.00	Bottom	2.00	3.50	0.57	1,714.29	1,714.29
					Cell Total Biomass Density (g/m2):	6,714.29	6,714.29

Reduction Cohort 2

Example D	Cohort Biomass Density (g/m2)	Layer	LAI	MaxLAI	Adjusted PCanArea	Cell Biomass Density (g/m2)	Layer Biomass Density (g/m2)
Cohort 1	10000.00	Top	3.50	3.50	0.50	5,000.00	-
Cohort 2	3000.00	Top	1.50	3.50	0.43	1,285.71	6,285.71
Cohort 3	3000.00	Bottom	2.00	3.50	0.57	1,714.29	1,714.29
					Cell Total Biomass Density (g/m2):	8,000.00	8,000.00

The distinction between cohort biomass density vs. cell-level biomass density is necessary to appropriately estimate cell-level biomass density as it would be empirically estimated in the field. If the biomass density was not rescaled within the layer, then biomass density would be overestimated (e.g., example B would be 23,000 g/m^2, i.e., the sum of the second column) by not recognizing that they are competing for horizontal growing space when sharing a layer.

Thus, given the assumption that cohorts within a layer do not physically share horizontal space (canopy shyness), a weighted average of the cohorts on the cell is the best way to represent an attribute at the cell level, and canopy proportion (PCanArea) is used as the weighting factor. Cell-level biomass density is computed by:

$$Biomass_{Cell} = \sum Biomass_i \times PCanArea_i$$

This method of scaling cohort-level densities to the cell scale applies to all values that are densities (unit/m^2), including all forms of biomass, non-structural carbon (reserves), LAI, photosynthetic output, respiration and senescence. Attributes that have only cell-level values and are not cohort-specific (e.g., leaf litter, coarse woody debris) are not averaged. Scaling using PCanArea is applied only when reporting cell-scale attributes to which cohort-scale values are contributing. These cell-scale averages (weighted by canopy proportions) are directly comparable to most empirical estimates of cohort attributes (Reese et al. in review, Gustafson et al. in review). In the cell-specific cohort log files produced by the PnET-Succession SiteOutput capabilities (see PnET-Succession v5.1 User Guide), canopy-weighted variable estimates (cell-level) have the string "Site" as a prefix in the column name, and cohort-level values lack the prefix. Thus, users who request such site-specific (cell-level) outputs (as is often done for calibration purposes) can access selected state variable values at both the cohort and cell level. All landscape-wide summary outputs report only cell-level (weighted) estimates as described above.

4.4 Defining cell-level initial conditions

When users choose to supply initial cohort biomass values along with cohort age, a 'spin-up' of initial biomass is not required. However, the proper assignment of such cohorts to a major canopy layer requires information about the maximum size that the cohort reached in its lifetime to preserve the integrity of the "biomass as a surrogate for height" assumption. The model therefore includes an option to invoke spin-up for the sole purpose of estimating maximum lifetime biomass, then replacing initial biomass value with the user-supplied value for the cohort's current biomass. The estimated maximum lifetime biomass value is then used to assign a cohort to a canopy layer by comparison to the maximum biomass of the other cohorts on the cell as described above (Section 4.2). Three options for assigning lifetime maximum biomass are available to the user (see User Guide). The first option uses the maximum biomass achieved during

spin-up for each cohort. The second option rescales the spin-up maximum biomass in proportion to the ending spin-up biomass as compared to the input biomass.

$$MaxBiomass = MaxBiomass_{SpinUp} \times \frac{Biomass_{Input}}{Biomass_{SpinUp}}$$

For example, if the Biomass$_{Input}$ was 500 g/m2, and the spin-up process resulted in an estimated cohort biomass of 2000 g/m2 and a MaxBiomass$_{SpinUp}$ of 2200 g/m2, the ratio of Biomass$_{SpinUp}$/Biomass$_{Input}$ is 500/2000 or 0.25. The MaxBiomass would be reduced proportionally using that ratio (2200 * 0.25 = 550). This approach effectively assumes that discrepancies between given cohort biomass and biomass estimated by spin-up reflect consistent growth differences for the cohort over its lifespan, and that its maximum biomass would be impacted by a similar proportion. The third option assumes the current biomass is the maximum biomass a cohort achieved in its life and spin-up is therefore not necessary.

Any cohort biomass values provided by the user in the initial conditions input file are assumed to be in units of cell-scale wood biomass density. The scaling of those units to cohort-level biomass density uses the inverse of the calculation above:

$$Biomass_i = \frac{Biomass_{Cell}}{PCanArea_i}$$

However, the actual value of PCanArea(i), must also be estimated and it is dependent on the LAI of the cohort and of any other cohorts in the same layer. This creates a circular calculation by attempting to estimate Biomass$_i$, LAI$_i$, and the resultant PCanArea$_i$ simultaneously. The model resolves this estimation through an iterative calculation and adjustment to cohort-level biomass density (Biomass$_i$), seeking the combination of cohort biomass and canopy proportion that results in a cell-level biomass value equivalent to the inputs for all cohorts in the initial community. This estimation procedure can sometimes fail to find a suitable solution for the first two methods for estimating lifetime maximum biomass, in which case it issues a warning and falls back on the third option of no spin-up.

4.5 Soil ice and waterlogging dynamics

Major revisions to the soil hydrology routines (v.4.0) allow simulation of waterlogged and swamp (standing water) soils, including over permafrost (Gustafson et al. 2020c). To support the latter, dynamic (monthly) calculation of the soil temperature profile is now an option. This allows the model to simulate ActiveLayerDepth (depth to the top of any ice layer in summer months) over permafrost (along with its effect on soil hydrology) and FrostDepth (depth to the bottom of any surface ice layer in winter months), and the model can pass soil temperature information to other extensions (e.g., Root Rot extension; Gustafson et al. 2022b) as needed. The soil temperature and

associated freezing and thawing dynamics in the soil profile are fully described in Gustafson et al. (2020c).

Standing water can be simulated using the ecoregion RunoffCapture parameter, which specifies the height above the soil surface that water can accumulate before any runoff occurs, representing the average height of basin outlets in the ecoregion (Gustafson et al. 2020c). This parameter is used to allow soil water to accumulate above saturation (i.e., flooded). RunoffCapture only applies to water that exceeds the soil porosity (saturation) and a value of zero causes any excess to all run off (previous version behavior). This excess water (above saturation) is retained in the soil "bucket" until interception, runoff, leakage (if any), evaporation, and transpiration collectively exceed cumulative precipitation inputs (i.e., consumed all excess water). Such oversaturated conditions induce waterlogging stress in species with little waterlogging tolerance (specified by the H1 and H2 parameters).

4.6 Albedo

PnET-succession v.5.1 includes an option to calculate monthly albedo as a function of snow cover and vegetation characteristics of boreal ecosystems. The algorithm to estimate monthly albedo from PnET-Succession state variables uses equations fitted to approximations of the empirical data (graphs) in Lukes et al. (2013), who measured albedo in pure boreal forest stands as a function of leaf area. Lower LAI means more of albedo is driven by the forest floor. Thus, the approach here is to compute albedo using the LAI of each canopy type on a cell to control for the effect of forest floor. The validity of this algorithm cannot be assumed for ecosystems other than boreal. The algorithm requires the LifeForm (canopy type) of each species. Currently valid types are dark conifer, light conifer, deciduous, ground cover (typically moss/lichen or grass), each representing different reflectivity properties (Lukes et al. 2013). In the following equations, y is albedo. Albedo units are DHR (directional hemispherical reflectance (black sky (shortwave) albedo), which is a ratio of reflected solar radiation to incoming solar radiation.

For dark (low reflectivity) conifers (Lukes et al. 2013),

$y = -0.067 * \ln(LAI) + 0.2095$

In the presence of snow (>10 cm), add 80% to the estimate (Betts and Ball 1997). Snow effect increases linearly as snow depth increases from 0 to 10 cm (for all life forms). Constrain LAI to be no less than 0.7 to prevent computations from extrapolating beyond the data.

For light (greater reflectivity) conifers (Lukes et al. 2013),

$y = -0.054 * \ln(LAI) + 0.2082$

In the presence of snow (>10 cm), add 75% to the estimate (Betts and Ball 1997). Constrain LAI to be no less than 0.7 for computations.

For deciduous, (Lukes et al. 2013),

y = -0.0073*LAI + 0.231

In the presence of snow, add 35% to the estimate (Betts and Ball 1997).

For Grass or moss or open (Betts and Ball 1997),

y = 0.24

In the presence of snow, add 312.5% to the estimate (y = 0.75) (Betts and Ball 1997).

Cell albedo (y) is computed as a weighted average in the topmost canopy layer having LAI>1, weighting by proportion of leaf area of each canopy type. Albedo is not estimated for non-active cells.

4.7 Other enhancements

Other general enhancements in v.5 include: 1) parallelization of cohort growth, including during spin-up. 2) A new PnET-Succession cohort library that moved code from the main body of code to a library to streamline the passing of state variables to and from other extensions and to make code maintenance more efficient. 3) Optional output maps of albedo (landscape reflectance) suited for boreal landscapes (section 4.6). 4) Optional maps of permafrost active layer depth (in summer) and frost depth (in winter) (section 4.5). 5) Options to read initial cohort biomass from the LANDIS-II initial conditions MapCode text file instead of using spin-up, with an additional option to read initial cohort biomass and run spin-up solely to determine the correct canopy layer assignment for each cohort (see section 4.2). 6) Options to output maps and tables of landscape averages through time of each individual biomass pool and selected combinations. Many state variables that are output as maps now also have a table generated containing average map values by timestep. 7) Additional state variables were added to the (optional) cell-level outputs (maps and tables) to enhance model diagnostics and troubleshooting.

5. Discussion

PnET-Succession was developed to provide more robust projections of forest landscape dynamics under novel conditions that have no scientifically studied analog, such as climate change, exotic invasive species and pests, and novel species assemblages such as those created by assisted migration. This was achieved by replacing phenomenological growth and competition algorithms with algorithms based on physical and physiological first principles as much as possible while keeping the model tractable for landscape spatial and temporal scales.

Earlier versions of PnET-Succession have proved useful in several studies of novel scenarios. A study of potential American chestnut (*Castanea dentata*) restoration showed that blight-resistant chestnuts are likely able to compete in the existing forests of western Maryland (USA), but that an aggressive restoration planting program would be required to restore it to something approaching its former dominance within this century (Gustafson et al. 2018b). The study also indicated that the large size and decay-resistance of chestnut would not appreciably increase the carbon sequestration potential of Appalachian forests. In a related study, Gustafson et al. (2022b) found that the fungal pathogen causing root rot (*Phytophthora cinnamomi*) would negatively impact chestnut restoration efforts, especially in locations south of 40° N.

PnET-Succession's mechanistic algorithms enabled the virtual extension of an 11-year Free Air Carbon Enrichment (FACE) experiment in northern Wisconsin (USA) investigating the effects of elevated CO_2 and ozone on the growth and competition of trees. The model was able to virtually extend the experiment for up to 150 years and to include some tree species from the region that were not part of the empirical experiment (Gustafson et al. 2018a). The model was then able to extend the experiment spatially to a 104,471 ha sub-boreal landscape containing 24 species not part of the empirical experiment (Gustafson et al. 2020a). In a more recent study, Gustafson et al. (2020b) used PnET-Succession to evaluate the effectiveness of various assisted migration strategies designed to adapt forest ecosystems to changing climate. These strategies planted novel species (translocated up to 500 km) following timber harvest events, and the mapped model outputs were summarized in terms of the supply of ecosystem goods and services through simulated time.

The innovations for version 5 described here are anticipated to greatly improve simulation of canopy dynamics, response to partial disturbance, water balance, and competitive interactions among tree species in response to changing environmental conditions and multiple disturbance types. Nonetheless, PnET-Succession is by no means fully developed or mature. There are compelling opportunities for improvement. Some of those opportunities include minor adjustments of the above design to further improve stand structural dynamics and competitive interactions among tree species cohorts. For example, the strict assumption that once a cohort achieves crown closure within a layer it is constrained to its canopy proportion as a maximum for its lifetime could be relaxed to enable canopy expansion appropriate to its respective stage of growth. Canopy status that is sometimes available within existing forest inventories could inform the assignment of canopy layers applied at initial conditions. But other opportunities for improvement may require major changes to the design presented here.

An important goal for the LANDIS-II modeling platform is to provide users with the ability to simulate all the important drivers of forest dynamics using available extensions. One important deficiency in PnET-Succession (and most LANDIS-II succession

extensions) is that soil nutrients are not directly limiting. Species productivity can be calibrated to chronically nutrient-poor ecoregions, but there is no dynamism in such an approach. There is a group of PnET and PnET-Succession developers actively collaborating to upgrade the PnET algorithms in PnET-Succession to add the capabilities of PnET-CN (Aber et al. 1997) to model nitrogen cycling (and nutrient limitations on growth) within PnET-Succession. Another task for this group is to find a way to enable foliage amount to be determined by light availability such that foliage allocation will cease when the carbon balance of additional foliage is negative. These algorithms exist in PnET-II, but creative thinking and testing is required to make them tractable in a landscape model with multiple cohorts on each cell. It is hoped that a release of at least the nitrogen capabilities can be achieved in 2023.

PnET-Succession carries state variables that open opportunities for more mechanistic seed dispersal methods. The only method currently available is the Ward dispersal method (Ward et al. 2004), which assumes an indeterminate seed rain from all species with likelihood of sufficient seed source reaching a cell diminishing with distance from the source using a double-exponential decline function. In this implementation, a successfully established cohort from seeding initializes with the same initial biomass regardless of the quantity and distance of seed sources. A more demographically based method is under development that estimates propagule pressure based on size of propagules, the abundance of the species within dispersal distance, and the distance propagules have traveled, with consequent differences in initial biomass among cohorts established from different seed sources.

6. Summary

PnET-Succession is a widely used succession extension for the LANDIS-II forest landscape model that has become poorly documented because the only description of its design and algorithms (de Bruijn et al. 2014) has gradually become obsolete. While the User Guide (Gustafson and Miranda 2022a) provides a succinct description of the model design and its basic algorithms that is updated with each version release, its purpose is to describe how to use the model and does not provide a comprehensive description of the algorithms and equations used in the computation of most state variables. In this paper we have provided the conceptual and computational details needed to understand the mathematical formulation of the model without having to study the source code. As such, this paper responds to the repeated calls for greater transparency in forest landscape models (Scheller 2018) and for ecological and environmental models more generally (Grimm et al. 2014).

Literature Cited

Aber J.D. and C.A. Federer. 1992. A generalized, lumped-parameter model of photosynthesis, evaporation and net primary production in temperate and boreal forest ecosystems. Oecologia 92:463–474.

Aber, J.D., S.V. Ollinger, C.A. Federer, et al. 1995. Predicting the effects of climate change on water yield and forest production in the northeastern United States. Climate Research 5:207-222.

Aber, J.D., P.B. Reich, M. Goulden. 1996 . Extrapolating leaf CO_2 exchange to the canopy: a generalized model of forest photosynthesis compared with measures by eddy correlation. Oecologia 106:257-265.

Aber, John D., Scott V. Ollinger, Charles T. Driscoll. 1997. Modeling nitrogen saturation in forest ecosystems in response to land use and atmospheric deposition. Ecological Modelling 101:61-78. DOI:10.1016/S0304-3800(97)01953-4.

Betts, Alan K. and John H. Ball. 1997. Albedo over the boreal forest. J. Geophysical Research 102(D24):28901-28909.

Brodribb, T.J., Powers, J., Cochard, H. and Choat, B. 2020. Hanging by a thread? Forests and drought. Science 368(6488):261-266.

de Bruijn A., E.J. Gustafson, B.R. Sturtevant, J.R Foster., B.R. Miranda, N.I. Lichti, D.F. Jacobs. 2014. Toward more robust projections of forest landscape dynamics under novel environmental conditions: embedding PnET within LANDIS-II. Ecological Modelling 287:44–57. DOI: 10.1016/j.ecolmodel.2014.05.004.

Fisher, R.A., C.D. Koven, W.R. Anderegg, B.O. Christoffersen, M.C. Dietze, C.E. Farrior, J.A. Holm, G.C. Hurtt, R.G. Knox, P.J. Lawrence, and J.W. Lichstein. 2018. Vegetation demographics in Earth System Models: A review of progress and priorities. Global Change Biology 24:35-54.

Franks P.J., M.A. Adams, J.S. Amthor, M.M. Barbour, J.A. Berry, D.S. Ellsworth, G.D. Farquhar, O. Ghannoum, J. Lloyd, N. McDowell, R.J. Norby, D.T. Tissue. S. von Caemmerer. 2013. Sensitivity of plants to changing atmospheric CO_2

concentration: from the geological past to the next century. New Phytologist 197:1077–1094. DOI: 10.1111/nph.12104.

Grimm, V., J. Augusiak, A. Focks, B.M. Frank, F. Gabsi, A.S.A. Johnston, C. Liu, B.T Martin, M. Meli, V. Radchuk, P. Thorbek, S.F. Railsback. 2014. Towards better modelling and decision support: Documenting model development, testing, and analysis using TRACE. Ecological Modelling 280:129-139.

Gustafson, E.J. 2013. When relationships estimated in the past cannot be used to predict the future: using mechanistic models to predict landscape ecological dynamics in a changing world. Landscape Ecology 28:1429-1437. DOI: 10.1007/s10980-013-9927-4.

Gustafson, Eric J., Mark E. Kubiske, Brian R. Miranda, Yasutomo Hoshika, Elena Paoletti. 2018a. Extrapolating plot-scale CO_2 and ozone enrichment experimental results to novel conditions and scales using mechanistic modeling. Ecological Processes 7:31. DOI: 10.1186/s13717-018-0142-8.

Gustafson, Eric J., A.M.G. de Bruijn, N. Lichti, D.F. Jacobs, B.R. Sturtevant, D.M. Kashian, B.R. Miranda, P.A. Townsend. 2018b. Forecasting effects of tree species reintroduction strategies on carbon stocks in a future without historical analog. Global Change Biology 24:5500–5517. DOI: 10.1111/gcb.14397.

Gustafson, Eric J., Brian R. Sturtevant, Brian R. Miranda. 2020a. Scaling Aspen-FACE plot-scale experimental results to landscape scale using a mechanistic forest landscape model. Ecosphere 11(6), e03162. DOI: 10.1002/ecs2.3162.

Gustafson, Eric J., Christel C. Kern, Brian R. Miranda, Brian R. Sturtevant, Dustin R. Bronson and John M. Kabrick. 2020b. Climate adaptive silviculture: how much will it take to produce resilient forest landscapes? Forest Ecology and Management Volumes 470–471:118208. DOI: 10.1016/j.foreco.2020.118208.

Gustafson Eric J., Brian R. Miranda, Anatoly Z. Shvidenko, Brian R. Sturtevant. 2020c. Simulating growth and competition on wet and waterlogged soils in a forest landscape model. Frontiers in Ecology and Evolution 8:598775. DOI: 10.3389/fevo.2020.598775.

Gustafson, E.J., and B.R. Miranda. 2022a. PnET-Succession v5.0 Extension User Guide. Published on the Internet by the LANDIS-II Foundation. URL: http://www.landis-ii.org/extensions/pnet-succession.

Gustafson Eric J., Brian R. Miranda, Tyler J. Dreaden, Cornelia C. Pinchot, Douglass F. Jacobs. 2022b. Beyond blight: *Phytophthora* root rot under climate change limits populations of reintroduced American chestnut. Ecosphere 13:e3917.

Gustafson, Eric J., Brian R. Sturtevant, Brian R. Miranda. in review. Overcoming conceptual hurdles to accurately represent trees as cohorts in forest landscape models. Ecological Modelling.

Hajek, Peter, Dominik Seidel, Christoph Leuschner. 2015. Mechanical abrasion, and not competition for light, is the dominant canopy interaction in a temperate mixed forest. Forest Ecology and Management 348:108-116. https://doi.org/10.1016/j.foreco.2015.03.019.

Hamon, W. R. 1961. Estimating potential evapotranspiration. Journal of the Hydraulics Division, 87, 107-120.

Huston, M. and Smith, T. 1987. Plant succession: life history and competition. The American Naturalist 130(2):168-198.

Kreuzweiser, J. and Rennenberg, H. 2014. Responses of tree to waterlogging. Plant, Cell and Environment 37: 2245-2259. https://doi.org/10.1111/pce.12310.

Jassby A.D. and Platt T. 1976. Mathematical formulation of the relationship between photosynthesis and light for phytoplankton. Limnology and Oceanography 21:540–547.

Lukeš Petr, Pauline Stenberg, Miina Rautiainen. 2013. Relationship between forest density and albedo in the boreal zone. Ecological Modelling 261–262:74-79. DOI: 10.1016/j.ecolmodel.2013.04.009.

Menezes-Silva, PE, Loram-Lourenço, L, Alves, RDFB, Sousa, LF, Almeida, SEDS, Farnese, FS. 2019. Different ways to die in a changing world: Consequences of climate change for tree species performance and survival through an ecophysiological perspective. Ecology and Evolution 9:11979–11999. https://doi.org/10.1002/ece3.5663.

Mundim, Kleber C., Solange Baraldi, Hugo G. Machado, Fernando M.C. Vieira. 2020. Temperature coefficient (Q10) and its applications in biological systems: Beyond the Arrhenius theory. Ecological Modelling 431:109127. DOI: 10.1016/j.ecolmodel.2020.109127.

Reese, G.C., Dymond C., Quigley, K., Duveneck M., Gustafson E., Scheller R.M. Lucash M., Russell M., Miranda B., Sturtevant B. In review. Application of growth and yield data and models to calibrate forest-landscape models. Canadian Journal of Forest Research.

Scheller, R. M. 2018. The challenges of forest modeling given climate change. Landscape Ecology 33(9):1481–1488. https://doi.org/10.1007/s10980-018-0689-x.

Scheller, R.M. and D.J. Mladenoff. 2004. A forest growth and biomass module for a landscape simulation model, LANDIS: Design, validation, and application. Ecological Modelling 180(1):211-229.

Scheller, R.M., J.B. Domingo, B.R. Sturtevant, J.S. Williams, A. Rudy, E.J. Gustafson, and D.J. Mladenoff. 2007. Design, development, and application of LANDIS-II, a spatial landscape simulation model with flexible temporal and spatial resolution. Ecological Modelling 201:409-419.

USDA Natural Resource Conservation Service. 2004. National Engineering Handbook - Part 630. Chapter 11: Snowmelt.

Ward, B.C., R.M. Scheller and D.J. Mladenoff. 2004. Technical Report: LANDIS-II double exponential seed dispersal algorithm. Published by the LANDIS-II Foundation. Available for download at https://www.landis-ii.org/users.

Weng E.S., S.Malyshev, , J.W.Lichstein, , C.E.Farrior, , R.Dybzinski, , T.Zhang, , E. Shevliakova, and S.W Pacala. 2015. Scaling from individual trees to forests in an Earth System Modeling framework using a mathematically tractable model of height-structured competition. Biogeosciences 12:2655-2694.

Wythers, K.R., P.B. Reich, J.B. Bradford. 2013. Incorporating temperature-sensitive Q10 and foliar respiration acclimation algorithms modifies modeled ecosystem responses to global change. Journal of Geophysical Research: BioGeosciences 118:1-14.

Xu, C., Gertner, G.Z. and Scheller, R.M. 2009. Uncertainties in the response of a forest landscape to global climatic change. Global Change Biology 15(1):116-131.

Appendix. Names, definitions and potential (N. American) sources for PnET-Succession input parameters. See main text, de Bruijn et al. (2014) and Gustafson and Miranda (2022a) for additional details about their function.

Name	Definition	Units	Source(s)
LANDIS-II Species parameters			
Longevity	Typical longevity (not record longevity)	years	Burns and Honkala 1990
Effective Seed Dispersal Distance	95% of seeds disperse within this distance	m	Various (by species)
Max Seed Dispersal Distance	Maximum dispersal distance	m	Various (by species)
Sprout probability	Probability that cohort will re-sprout if killed	probability	Burns and Honkala 1990
Min sprout age	Age below which a killed cohort will not resprout	years	Burns and Honkala 1990
Max sprout age	Age above which a killed cohort will not resprout	years	Burns and Honkala 1990
PnET-Succession Species parameters			
FolN	Foliar nitrogen	% by weight	Serbin et al. 2014, Ryu et al. 2008, Reich et al. 1995
SLWmax	Maximum specific leaf weight at the top of canopy	(g/m^2)	Serbin et al. 2014, Ryu et al. 2008, Abrams and Kubiske 1990
SLWDel	Rate of change in specific leaf weight from top to bottom of canopy	proportion	Aber et al. 1995
k	Canopy light attenuation constant (light extinction coefficient)	None	Aber et al. 1995
AmaxA	Intercept of relationship between foliar N and maximum net photosynthetic rate	μmol $CO_2/g/s$	Aber et al. 1995
AmaxB	Slope of relationship between foliar N and maximum net photosynthetic rate	μmol $CO_2/g/s$	Aber et al. 1995
FracFol	Fraction of the amount of active woody biomass that determines allocation to foliage	Proportion per year	Tuned
FrActWd	Shape parameter controlling the fraction of woody biomass containing active xylem capable of supporting foliage	None	Tuned
TOFol	Turnover of foliage (foliage biomass lost annually)	Proportion per year	Burns and Honkala 1990, Barnes and Wagner 1981
TOwood	Wood turnover (loss to breakage, self-thinning, etc.)	Proportion per year	De Bruijn et al. 2014
TOroot	Root turnover (loss to breakage, damage, etc.)	Proportion per year	De Bruijn et al. 2014
BFolResp	Base foliar respiration (proportion of maximum photosynthetic rate)	Proportion	De Bruijn et al. 2014

MaintResp	Maintenance respiration (proportion total biomass)	Proportion	Tuned
HalfSat	Half saturation light level for photosynthesis	μmol/m2/sec	Ryu et al. 2008, Niinemets and Valladares 2006
H1	Waterlogging stress: pressure head at which phototsynthesis stops	m pressure head	Kattge 2019
H2	Waterlogging stress: pressure head at which phototsynthesis begins to decline	m pressure head	Kattge 2019
H3	Water stress: pressure head at which phototsynthesis begins to decline	m pressure head	Kattge 2019
H4	Water stress: pressure head at which phototsynthesis stops	m pressure head	Kattge 2019
PsnTMin	Minimum temperature for photosynthesis	^{O}C-avg. daytime temperature	Gustafson and Miranda 2022a
PsnTOpt	Optimum temperature for photosynthesis	^{O}C-avg. daytime temperature	Gustafson and Miranda 2022a
PsnTMax	Maximum temperature for photosynthesis	^{O}C-avg. daytime temperature	Gustafson and Miranda 2022a
PsnAgeRed	Shape parameter controlling rate of senescence	None	De Bruijn et al. 2014
FracBelowG	Fraction of non-foliar biomass that is belowground (root pool)	Proportion	Martin et al. 1998
EstMoist	Scaling parameter to weight the effect of soil moisture on establishment	None	Gustafson and Miranda 202a2
EstRad	Scaling parameter to weight the effect of light on establishment	None	Gustafson and Miranda 2022a
KWdLit	Decomposition rate (decay constant, k) of woody litter	Proportion per year	Mattson et al. 1987
FolLignin	Mass fraction of lignin in foliage tissue	Proportion or g/g	Aber and Mellilo 1982, Nowacki and Abrams 2008, Cromack and Monk 1975
DNSC	Target proportion of carbon reserves relative to total active biomass	Proportion	De Bruijn et al. 2014
Site-level parameters			
MaxCanopyLayers	Maximum number of canopy layers allowed	Count	Expert judgement
LayerThreshRatio	When biomass of cohorts varies by more than this value, they will be placed in different canopy layers	Ratio	Expert judgement
MaxPest	Tune establishment probability of all species together	Ratio	Tuned
EvapDepth	Maximum soil depth that evaporation occurs	mm	Expert judgement

Literature Cited - Appendix

Aber, J. D., and J. M. Melillo. 1982. Nitrogen immobilization in decaying hardwood leaf litter as a function of initial nitrogen and lignin content. Canadian Journal of Botany 60:2263-2269.

Aber, J. D. et al. 1995. Predicting the effects of climate change on water yield and forest production in the northeastern United States. Climate Research 5:207-222.

Abrams, M. D., and M. E. Kubiske. 1990. Photosynthesis and water relations during drought in Acer rubrum L. genotypes from contrasting sites in central Pennsylvania. Functional Ecology 4:727–733.

Barnes, B. V., and W. H. Wagner Jr. 1981. Michigan trees: A guide to the trees of Michigan and the Great Lakes Region. Univ. of Michigan Press, Ann Arbor, MI, USA.

Burns R. M, and Honkala B.H., tech. coords. 1990. Silvics of North America: 1. Conifers; 2. Hardwoods. Agriculture Handbook 654. U. S. Dept of Agriculture, Forest Service, Washington, DC, USA.

Cromack, K. Jr., and C. D. Monk. 1975. Litter production, decomposition, and nutrient cycling in a mixed hardwood watershed and a white pine watershed. Pp. 609-624 in: Howell, F.G., J. B. Gentry, and M. H. Smith. (eds), Mineral Cycling in Southeastern Ecosystems. USDC National Technical Information Service, Springfield, Virginia, USA.

de Bruijn, A., E. J. Gustafson, B. R. Sturtevant, J. R. Foster, B. R. Miranda, N. I. Lichti, and D. F. Jacobs. 2014. Toward more robust projections of forest landscape dynamics under novel environmental conditions: embedding PnET within LANDIS-II. Ecological Modelling 287:44–57.

Gustafson, E.J., and B.R. Miranda. 2022a. PnET-Succession v5.1 Extension User Guide. Published on the Internet by the LANDIS-II Foundation. URL: http://www.landis-ii.org/extensions/pnet-succession

Kattge, J., Bönisch, G., Diaz, S., Lavorel, S., Prentice, I. C., Leadley, P., … Wirth, C. 2019. TRY plant trait database – enhanced coverage and open access. Glob Change Biol. https://doi.org/10.1111/gcb.14904

Martin, J. G., B. D. Kloeppel, T. L. Schaefer, D. L. Kimbler, and S. G. McNulty. 1998. Aboveground biomass and nitrogen allocation of ten deciduous southern Appalachian tree species. Canadian Journal of Forest Research 28:1648-1659.

Mattson, K., W. T. Swank, and J. B. Wade. 1987. Decomposition of woody debris in a regenerating, clear-cut forest in the Southern Appalachians. Canadian Journal of Forest Research 17:712-721.

Niinemets, Ü., F. Valladares. 2006. Tolerance to shade, drought, and waterlogging of temperate Northern Hemisphere trees and shrubs. Ecological Monographs 76:521–547.

Nowacki, G. J., and M. D. Abrams. 2008. The demise of fire and "mesophication" of forests in the eastern United States. BioScience 58:123-138.

Reich, P. B., M. B. Walters, B.D. Kleppel, and D. S. Ellsworth. 1995. Different photosynthesis-nitrogen relations in deciduous hardwood and evergreen coniferous tree species. Oecologia 104:24-30.

Ryu, S-R., J. Chen, A. Noormets, M. K. Bresee, and S. V. Ollinger. 2008. Comparisons between PnET-Day and eddy covariance based gross ecosystem production in two Northern Wisconsin forests. Agricultural and Forest Meteorology 148:247–256.

Serbin, S. P., A. Singh, B. E. McNeil, C. C. Kingdon, and P. A. Townsend. 2014. Spectroscopic determination of leaf morphological and biochemical traits for northern temperate and boreal tree species. Ecological Application 24:1651–1669.